Core excitation effects in the breakup of the one-neutron halo nucleus ^{11}Be on a proton target

A. M. Moro[1,*] and R. Crespo[2,3,†]

[1]*Departamento de Física Atómica, Molecular y Nuclear, Universidad de Sevilla, Apartado 1065, E-41080 Sevilla, Spain*
[2]*Centro de Física Nuclear, Universidade de Lisboa, Avenida do Professor Gama Pinto 2, P-1649-003 Lisboa, Portugal*
[3]*Departamento de Física, Instituto Superior Técnico, Universidade Técnica de Lisboa, Avenida do Professor*
Cavaco Silva, Taguspark, P-2780-990, Oeiras, Portugal

We investigate the phenomenon of core excitation in the inelastic and breakup of two-body halo nuclei, composed by a valence nucleon and a core. To evaluate the importance of this effect we propose a simple reaction model based on an extension of the standard distorted wave Born approximation (DWBA) method. The model takes into account core-excited admixtures in the states of the composite projectile, as well as the possibility of dynamic core excitation due to the interaction of the core with the target. As an application of the model, we present calculations for the breakup of ^{11}Be on a proton target at an incident energy of 63.7 MeV/nucleon, comparing it with the available data for this reaction. We find that the data are well reproduced by the model and that the effect of dynamic core excitation is essential to explain the observed cross section.

I. INTRODUCTION

Breakup and inelastic scattering are now standard techniques to study the structure of halo nuclei. In particular, the proton target is very appealing for spectroscopic studies because the excitation occurs mainly due to the nuclear interaction, thereby exciting several multipolarities and revealing the resonant structure of the projectile continuum [1,2]. To extract reliable information from these data it is important to identify the relevant excitation mechanisms. In the case of a projectile composed by a valence particle weakly bound to a core, it is commonly assumed that the main excitation mechanism is due to the excitation of the valence nucleon outside the core. This single-particle picture is behind many few-body reaction formalisms used in the analysis of reactions induced by halo and other weakly bound nuclei, such as the continuum-discretized coupled-channels (CDCC) method [3], the adiabatic approximation [4,5], the Alt, Grassberger, Sandhas (AGS) formulation of the Faddeev equations [6,7], and a variety of semiclassical approaches [8–13].

Despite the relative success of these methods, they typically ignore the fact that the projectile states will contain, in general, significant admixtures of several core components and, therefore, the excitation of the projectile may be caused also by transitions between these core states.

These effects are not included in the standard formulations of the methods discussed above, although some efforts have been made in recent years toward this direction. A recent example is the extended version of the CDCC method (named XCDCC) recently proposed by the authors of Ref. [14].

The effect of core excitation has also been studied [15], using an extension of the adiabatic model of Ref. [16]. The formalism was applied to the elastic scattering of ^{8}B on a

carbon target, and some contribution was found at large angles due to the excitation of the ^{7}Be core.

It is the purpose of this work to evaluate the influence of these core excitation effects in the inelastic and breakup of halo nuclei using a simple model, but retaining nevertheless the key physics. The model presented here is an extension of the core excitation model presented in a previous work [17]. Under the assumption that the DWBA approximation is valid, and that core-recoil effects can be neglected, this model gives a simple relation between the excitation of the projectile and that of the core on the same target. The model was applied to the breakup of ^{11}Be on a proton target at 63.7 MeV/nucleon incident energy, and compared with the data from Ref. [1]. Due to the experimental energy resolution, the experimental angular distributions for the exclusive breakup were extracted for two intervals of neutron-^{10}Be core energy: (i) $E_{\rm rel} = 0$–2.5 MeV and (ii) $E_{\rm rel} = 2.5$–5.0 MeV. In the first interval one expects an important contribution coming from the low-lying narrow $5/2^+$ resonance at a relative energy of 1.28 MeV [18]. This resonance has a dominant ^{10}Be$(0^+) \otimes \nu 1d_{5/2}$ parentage and a small component ^{10}Be$(2^+) \otimes \nu 2s_{1/2}$. The cross section for the second interval contains, presumably, contributions coming from several resonances, namely, $E_x = 2.64$ MeV ($3/2^-$), 3.40 MeV ($3/2^-$, $3/2^+$), 3.89 MeV ($5/2^-$), and 3.95 ($3/2^-$) [18]. In a previous work, we analyzed these data using a simple version of the core excitation model [17], and showed that the main contribution to the second interval comes from the resonance at 3.40 MeV, for which we assumed a $3/2^+$ assignment, following the suggestion of the authors of Ref. [19]. These calculations provided a reasonable agreement with the data of Ref. [1] and, most importantly, evidenced the importance of the core excitation mechanism in the breakup of halo nuclei.

The calculations performed by the authors of Ref. [17] assumed a simple single-particle configuration for the valence neutron in the ^{11}Be nucleus relative to the ^{10}Be core. It is the purpose of this work to extend this model to the more

―――――――
*moro@us.es
†raquel.crespo@ist.utl.pt

realistic situation in which the projectile states consist of a superposition of different valence configurations and core states.

The paper is structured as follows. In Sec. II we introduce the Hamiltonian used in this work. In Sec. III, we describe the core excitation reaction model used in the scattering calculations. In Sec. IV we detail the structure model used to describe the ^{11}Be states. In Sec. V we present the calculations for the ^{11}Be + p reaction. Finally, Sec. VI is left for summary and conclusions.

II. THE FEW-BODY HAMILTONIAN

The three-body Hamiltonian for the system has the form

$$H = T_R + H_{\text{proj}} + V_{ct} + V_{vt}, \qquad (1)$$

where T_R represents the kinetic energy operator for the projectile-target relative motion, V_{ct} and V_{vt} are the core-target and the valence-target interactions, and H_{proj} is the internal Hamiltonian of the projectile, given by

$$H_{\text{proj}} = T_r + V_{vc}(\vec{r}, \vec{\xi}) + h_{\text{core}}(\vec{\xi}), \qquad (2)$$

where $\vec{r}$ is the relative coordinate between the valence and the core, T_r the core-valence kinetic energy operator, and $h_{\text{core}}(\vec{\xi})$ the intrinsic Hamiltonian of the core, whose energies and eigenstates are labeled by the angular momentum (I) and its projection (M_c), that is,

$$h_{\text{core}}|\Phi_{IM_c}\rangle = \varepsilon_I |\Phi_{IM_c}\rangle. \qquad (3)$$

Additional quantum numbers, required to fully specify the core states, are omitted for simplicity in the notation. The core-valence and core-target interactions may depend upon the internal core degrees of freedom $\vec{\xi}$. A given projectile state with total angular momentum and projection JM will consist on a linear superposition of several valence-core configurations

$$\Psi_{JM}(\vec{r}, \vec{\xi}) = \sum_{\alpha = I, \ell, j} \left[\psi_\alpha^J(\vec{r}) \otimes \Phi_I(\vec{\xi}) \right]_{JM}, \qquad (4)$$

where $\psi_\alpha^J(\vec{r})$ are wave functions describing the motion of the valence neutron relative to a given core state. The set of quantum numbers s, ℓ, and j refer to the intrinsic spin of the valence particle, its orbital angular momentum relative to the core, and their sum, respectively.

The wave functions $\psi_\alpha^J(\vec{r})$ will depend upon the adopted structure model. For our case study this will be described in Sec. IV.

III. THE REACTION APPROACH: CORE EXCITATION REACTION MODEL

In this section we report in detail the core-excited reaction formalism (C-ex) that shall be used to describe the excitation of a projectile nucleus (p), from its ground state with total angular momentum J to a final state J' due to its interaction with a target (t). The projectile nucleus is assumed to be well described by a valence particle (v) orbiting around a core of nucleons (c). The target is assumed to be inert. In our
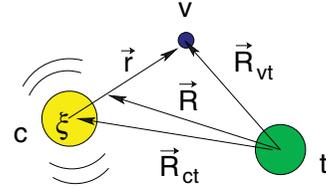

FIG. 1. (Color online) Relevant coordinates for the scattering of a two-body system, composed of a core (c) and a valence particle (v), scattered off a target nucleus (t).

working example, this will correspond to the excitation of ^{11}Be (^{10}Be + n) on a proton target to final states in the continuum, but the formalism could be equally applied to the transition between bound states. For simplicity, here we ignore the spin of the proton target.

The differential cross section for the excitation from an initial state $|\Psi_{JM}^i\rangle$ to a final state $|\Psi_{J'M'}^f\rangle$ of the projectile is given in general by

$$\frac{d\sigma_{pt}}{d\Omega} = \frac{1}{\hat{J}^2} \frac{\mu_{pt}}{(2\pi\hbar^2)^2} \frac{K'}{K} \sum_{M', M} \left| T_{pt}^{JM, J'M'} \right|^2 \qquad (5)$$

with $\hat{J} = \sqrt{2J+1}$, μ_{pt} is the projectile-target reduced mass, $\vec{K}$ ($\vec{K}'$) the initial (final) linear momentum, and $T_{pt}^{JM, J'M'}$ is the transition amplitude. Within the DWBA approach, the latter is given by

$$T_{pt}^{JM, J'M'} = \langle \chi_{\vec{K}'}^{(-)}(\vec{R}) \Psi_{J'M'}^f(\vec{r}, \vec{\xi}) | V_T | \chi_{\vec{K}}^{(+)}(\vec{R}) \Psi_{JM}^i(\vec{r}, \vec{\xi}) \rangle, \quad (6)$$

where $\chi_{\vec{K}}^{(+)}(\vec{R})$ and $\chi_{\vec{K}'}^{(-)}(\vec{R})$ are distorted waves describing the projectile-target relative motion in the initial and final channels, respectively. In a core + valence model of the projectile, the transition potential is

$$V_T = V_{vt}(\vec{R}_{vt}) + V_{ct}(\vec{R}_{ct}, \vec{\xi}), \qquad (7)$$

where $V_{vt}(\vec{R}_{vt})$ and $V_{ct}(\vec{R}_{ct}, \vec{\xi})$ are the valence-target and core-target potentials. The relevant coordinates for this problem are depicted in Fig. 1.

The valence-target interaction is assumed to be central, and hence $V_{vt}(\vec{R}_{vt}) = V_{vt}(R_{vt})$. On the other hand, the core-target interaction contains both central and noncentral parts, and is written as the multipolar expansion

$$V_{ct}(\vec{R}_{ct}, \vec{\xi}) = \sum_{\mathcal{L}, M} V_{ct}^{(\mathcal{L})}(R_{ct}, \xi) Y_{\mathcal{L}M}^*(\hat{R}) Y_{\mathcal{L}M}(\hat{\xi}). \qquad (8)$$

We assume that the radial form factor does not depend on the internal coordinates of the core [i.e., $V_{\mathcal{L}}(R_{ct}, \xi) = V_{\mathcal{L}}(R_{ct})$], which is valid for the rotational model used here.

From Eqs. (6) to (8) the DWBA amplitude is expressed as a sum of two terms:

$$T_{pt}^{JM, J'M'}(\vec{K}', \vec{K}) = T_{\text{val}}^{JM, J'M'} + T_{\text{corex}}^{JM, J'M'}. \qquad (9)$$

The first term, that we denote *valence amplitude* for shortness, is explicitly given by

$$T_{\text{val}}^{JM, J'M'}(\vec{K}', \vec{K}) = \langle \chi_{\vec{K}'}^{(-)}(\vec{R}) \Psi_{J'M'}^f(\vec{r}, \vec{\xi}) | V_{vt}(R_{vt}) $$
$$+ V_{ct}^{(0)}(R_{ct}) | \chi_{\vec{K}}^{(+)}(\vec{R}) \Psi_{JM}^i(\vec{r}, \vec{\xi}) \rangle. \quad (10)$$

This term contains only the central parts of the fragment-target potentials V_{vt} and V_{ct} and therefore it cannot induce transitions involving excitations of the core. Using the general form (4) for the initial and final states, this amplitude can be rewritten as

$$T_{\mathrm{val}}^{JM,J'M'}(\vec{K}',\vec{K}) = \sum_{\alpha,\alpha'} \langle \chi_{\vec{K}'}^{(-)}(\vec{R})\psi_{\alpha'}^{J'}(\vec{r}) | V_{vt}(R_{vt})$$
$$+ V_{ct}^{(0)}(R_{ct}) | \chi_{\vec{K}}^{(+)}(\vec{R})\psi_{\alpha}^{J}(\vec{r}) \rangle \delta_{I,I'}. \quad (11)$$

For each state I of the core contained in both the initial and final states of the projectile, this amplitude is similar to that found in conventional CDCC calculations and therefore can be evaluated using the standard codes available for this kind of calculations.

The second term of the transition amplitude is due to the noncentral part of the core interaction, that is,

$$T_{\mathrm{corex}}^{JM,J'M'}(\vec{K}',\vec{K}) = \sum_{\mathcal{L}>0,\mathcal{M}} \langle \chi_{\vec{K}'}^{(-)}(\vec{R})\Psi_{J'M'}^{f}(\vec{r},\vec{\xi}) | V_{ct}^{(\mathcal{L})}(R_{ct})$$
$$\times Y_{\mathcal{L}M}^{*}(\hat{R}_{ct})Y_{\mathcal{L}M}(\hat{\xi}) | \chi_{\vec{K}}^{(+)}(\vec{R})\Psi_{JM}^{i}(\vec{r},\vec{\xi}) \rangle. \quad (12)$$

This term accounts for the dynamic excitation of the core during the collision. It is the purpose of the present work to evaluate this term approximately, but retaining the key physics, to provide a simple estimation of the core excitation effects.

In addition to the core excitation mechanism, the amplitude (12) may also produce excitations in the core-valence relative motion. This is because the transition potential is evaluated at $\vec{R}_{ct}$. This coordinate can be expressed as $\vec{R}_{ct} = \vec{R} + \gamma\vec{r}$ $[\gamma = m_v/(m_v + m_c)]$. The dependence on the core-valence coordinate ($\vec{r}$) produces a core-recoil effect that can induce excitations of the projectile. However, because in our test case $\gamma \ll 1$, we will assume that this effect can be neglected in this amplitude [although it is fully taken into account in the amplitude (11)], so we can make the approximation $\vec{R} \approx \vec{R}_{ct}$ in Eq. (12), which means that the distorted waves in Eq. (12) are evaluated at the $\vec{R}_{ct}$ coordinate. This approximation leads to what we shall call hereafter the core excitation (C-exc) reaction model. We note that this model can be deduced from the XCDCC formalism [14] by calculating the transition in the Born approximation and neglecting the core-recoil effects for $\mathcal{L} > 0$.

The scattering amplitude for the C-exc approach factorizes then into a sum of products of a reaction and a structure term

$$T_{\mathrm{corex}}^{JM,J'M'} = \sum_{\mathcal{L}>0,\mathcal{M}} \mathcal{T}_{\mathcal{L}M}(\vec{K}',\vec{K})$$
$$\times \langle \Psi_{J'M'}^{f}(\vec{r},\vec{\xi}) | Y_{\mathcal{L}\mathcal{M}}(\hat{\xi}) | \Psi_{JM}^{i}(\vec{r},\vec{\xi}) \rangle, \quad (13)$$

where we have introduced the quantities

$$\mathcal{T}_{\mathcal{L}M}(\vec{K}',\vec{K}) = \langle \chi_{\vec{K}'}^{(-)}(\vec{R}_{ct}) | V^{(\mathcal{L})}(R_{ct})Y_{\mathcal{L}M}^{*}(\hat{R}_{ct}) | \chi_{\vec{K}}^{(+)}(\vec{R}_{ct}) \rangle, \quad (14)$$

which contain the dependence on the *reaction* part of the transition amplitude.

Using the Wigner-Eckart theorem in the form [20], we can write for the structure component

$$\langle \Psi_{J'M'}^{f} | Y_{\mathcal{L},M}(\hat{\xi}) | \Psi_{JM}^{i} \rangle = \langle J'M' | JM\mathcal{L}M \rangle \langle \Psi_{J'}^{f} || Y_{\mathcal{L}}(\vec{\xi}) || \Psi_{J}^{i} \rangle. \quad (15)$$

Noting that the operator appearing in the reduced matrix element depends only on the core coordinates and that the initial and final states are expressed in the form (4), this matrix element can be written as (see, for instance, Ref. [20], Appendix VI)

$$\langle \Psi_{J'}^{f} || Y_{\mathcal{L}}(\vec{\xi}) || \Psi_{J}^{i} \rangle = \sum_{\alpha,\alpha'} \langle R_{\alpha'}^{J'} | R_{\alpha}^{J} \rangle G_{\alpha J,\alpha' J'}^{(\mathcal{L})} \langle I' || Y_{\mathcal{L}}(\vec{\xi}) || I \rangle, \quad (16)$$

where we introduced the geometric factor

$$G_{\alpha J,\alpha' J'}^{(\mathcal{L})} = \delta_{j,j'}(-1)^{\mathcal{L}+j+J'+I}\hat{J}\hat{I}' \begin{Bmatrix} J' & J & \mathcal{L} \\ I & I' & j \end{Bmatrix}. \quad (17)$$

The reduced matrix element $\langle I' || Y_{\mathcal{L}}(\vec{\xi}) || I \rangle$ appearing in Eq. (16) depends on the structure model assumed for the core and will be specified later. Collecting results, the scattering amplitude for the core excitation reads

$$T_{\mathrm{corex}}^{JM,J'M'} = \sum_{\mathcal{L}>0,\mathcal{M}} \langle JM\mathcal{L}M | J'M' \rangle \mathcal{T}_{\mathcal{L}M}(\vec{K}',\vec{K})$$
$$\times \sum_{\alpha,\alpha'} \langle R_{\alpha'}^{J'} | R_{\alpha}^{J} \rangle G_{\alpha J,\alpha' J'}^{(\mathcal{L})} \langle I' || Y_{\mathcal{L}}(\vec{\xi}) || I \rangle. \quad (18)$$

The different terms that enter in this transition amplitude are relatively straightforward to calculate. The amplitudes $\mathcal{T}_{\mathcal{L}M}(\vec{K}',\vec{K})$, defined by Eq. (14), are those appearing in standard DWBA calculations with local form factors, for example, in inelastic scattering calculations. The radial functions $R_{\alpha}^{J}(r)$ are the solution of a coupled set of differential equations and the techniques to solve this problem are described elsewhere (see, e.g., the Appendix VI of Ref. [21]). The rest of the terms are just kinematical and geometrical factors.

The amplitude (18) can also be related to the two-body inelastic amplitudes for a core-target scattering problem. To make this relation explicit, let us consider a given transition $IM_c \to I'M_c'$ for the inelastic excitation of the core scattered off the same target. In DWBA, the amplitude for this process reads, similarly to Eq. (6),

$$T_{ct}^{IM_c,I'M_c'} = \langle \chi_{\vec{K}'}^{(-)}(\vec{R}_{ct})\Phi_{I'M_c'}^{f}(\vec{\xi}) | V_{ct}(\vec{R}_{ct},\vec{\xi}) |$$
$$\times \chi_{\vec{K}}^{(+)}(\vec{R}_{ct})\Phi_{IM_c}^{i}(\vec{\xi}) \rangle. \quad (19)$$

Using the Wigner-Eckart theorem, this amplitude can be also written as

$$T_{ct}^{IM_c,I'M_c'} = \langle I'M_c' | IM_c\mathcal{L}\mathcal{M} \rangle \widetilde{T}_{ct}^{(\mathcal{L}M)}(I \to I'), \quad (20)$$

with the *reduced amplitudes*

$$\widetilde{T}_{ct}^{(\mathcal{L}M)}(I \to I') = \mathcal{T}_{\mathcal{L}M}(\vec{K}',\vec{K})\langle I' || Y_{\mathcal{L}}(\hat{\xi}) || I \rangle, \quad (21)$$

with $\mathcal{T}_{\mathcal{L}M}(\vec{K}',\vec{K})$ given by Eq. (14).

Comparing with Eq. (18) and making use again of the no-recoil approximation ($\vec{R}_{ct} \approx \vec{R}$) we get the relation

$$
\begin{aligned}
T_{\text{corex}}^{JM,J'M'} &= \sum_{\mathcal{L}>0,\mathcal{M}} \langle J'M'|JM\mathcal{L}\mathcal{M}\rangle \\
&\times \sum_{\alpha,\alpha'} \langle R_{\alpha'}^{J'}|R_{\alpha}^{J}\rangle G_{\alpha J,\alpha' J'}^{(\mathcal{L})} \widetilde{T}_{\text{ct}}^{(\mathcal{L}\mathcal{M})}(I \to I'). \quad (22)
\end{aligned}
$$

This amplitude is equivalent to that given by Eq. (18), but emphasizes in a clear way the relation between the three-body scattering amplitude, Eq. (12), and the corresponding two-body amplitudes, under the approximations assumed by the model. Equation (22) provides also a practical way to numerically implementing the core-excited model since the two-body amplitudes can be obtained from any standard DWBA code.

In the extreme situation in which the valence excitation is small compared with the core excitation mechanism, the transition amplitude is given entirely by Eq. (18) and the corresponding cross section is obtained inserting this amplitude into Eq. (5). Furthermore, if there is a contribution from a single multipole transition $\mathcal{L}$, and a single configuration in the initial and final states, the projectile-target cross section becomes proportional to the cross section for the excitation of the core multiplied by a geometric factor and the radial overlap, that is,

$$
\left. \frac{d\sigma_{pt}}{d\Omega} \right|_{\text{corex}} = \frac{\hat{j}'^2}{\hat{j}^2} \frac{\hat{I}^2}{\hat{I}'^2} \left| G_{\alpha J,\alpha' J'}^{(\mathcal{L})} \langle R_{\alpha'}^{J'}|R_{\alpha}^{J}\rangle \right|^2 \frac{d\sigma_{ct}}{d\Omega}(I \to I'). \quad (23)
$$

This particular case was used in a preliminary application of this model to ^{11}Be $+ p$ resonant breakup [17].

Note, however, that in general both the valence and the core excitation mechanisms will contribute to the breakup process. In this case, the corresponding amplitudes need to be added coherently and hence interference effects will arise. In the present work we take into account simultaneously the valence and core excitation contributions.

IV. STRUCTURE MODEL

To calculate the initial and final states of the projectile one needs to specify the structure model for the core. In the calculations presented in this work for the ^{11}Be $+ p$ system, the projectile is treated within the particle-rotor model of Bohr and Mottelson [21]. Then we assume a rotational model for the ^{10}Be core with a permanent quadrupole deformation, which, for simplicity, is taken to be axially symmetric. Therefore, we can characterize the deformation by a single parameter β_2. In the body-fixed frame, the surface radius is then parametrized as $R(\hat{\xi}) = R_0[1 + \beta_2 Y_{20}(\hat{\xi})]$, with R_0 an average radius, to be specified later. Starting from a central potential, $V_{vc}^{(0)}(r)$, the full valence-core interaction is obtained by deforming this central interaction

$$
V_{vc}(\vec{r}, \hat{\xi}) = V_{vc}^{(0)}[r - \delta_2 Y_{20}(\hat{\xi})], \quad (24)
$$

with $\delta_2 = \beta_2 R_0$ being the deformation length. Transforming to the space-fixed frame of reference, and expanding in spherical

harmonics, this *deformed* potential reads

$$
V_{vc}(\vec{r}, \vec{\xi}) = \sum_{\mathcal{L},M} V_{vc}^{(\mathcal{L})}(r) Y_{\mathcal{L}M}^*(\hat{r}) Y_{\mathcal{L}M}(\hat{\xi}). \quad (25)
$$

The internal states of the projectile are expanded according to Eq. (4). If we write $\psi_\alpha^J(\vec{r}) = R_\alpha^J(r)\mathcal{Y}_{\ell s j m}(\hat{r})$, with $\mathcal{Y}_{\ell s j m}(\hat{r}) = [Y_\ell(\hat{r}) \otimes \chi_s]_{jm}$, the projectile states become

$$
\Psi_{JM}(\vec{r}, \vec{\xi}) = \sum_\alpha R_\alpha^J(r)[\mathcal{Y}_{\ell s j}(\hat{r}) \otimes \Phi_I(\vec{\xi})]_{JM}. \quad (26)
$$

The radial functions $R_\alpha^J(r)$ are then obtained by solving the Schrödinger equation using the potential (25) and with the appropriate boundary conditions.

For bound states, these radial functions decay exponentially for $r \to \infty$ giving rise to square-integrable functions. For continuum states, the functions $R_\alpha^J(r)$ are also obtained by solving a set of coupled radial equations, but subject to the boundary condition that incident waves occur in a given open channel characterized by a set of quantum numbers $\alpha = \{\ell, s, j, I\}$.

Although the calculations presented in this work could be performed with the scattering states themselves, it is numerically advantageous to adopt a *binning* procedure, similar to that used in CDCC calculations. Then, the continuum spectrum is divided into energy intervals. For each energy interval, or bin, a representative square-integrable state is constructed by a weighted superposition of scattering states within the bin interval. The bin wave function for a given incoming wave α is given by a square-integrable function, with a structure similar to that of the bound states (26)

$$
\begin{aligned}
\Psi_{[k_1 k_2]\alpha JM}^{\text{bin}}(\vec{r}, \vec{\xi}) &= \sum_{\alpha'} R_{[k_1 k_2]\alpha\alpha'}^{J}(r) \\
&\times [\mathcal{Y}_{\ell' s j'}(\hat{r}) \otimes \Phi_{I'}(\vec{\xi})]_{JM}, \quad (27)
\end{aligned}
$$

where $[k_1 k_2]$ denotes the momentum interval defining the bin.

V. APPLICATION TO ^{11}Be $+ p$ RESONANT BREAKUP

We now apply the core-excited model to the breakup of ^{11}Be on a proton target and compare with the data of [1]. Before presenting the calculations with this model, we consider the case ignoring the effect of deformation in both the ^{11}Be structure and in the core-target interaction.

A. Calculations without deformation

The calculations with no-deformation were done with the standard CDCC method, using the FRESCO code [22]. These calculations are similar to those presented in our previous work [23]. The valence-core interaction contains central + spin-orbit terms, of Woods-Saxon shape, with parameters adjusted to reproduce the ground state separation energy, the bound excited state $(1/2^-)$, and the position of the low-lying $5/2^+$ resonance. The core-target interaction corresponds to the Watson parametrization of Ref. [24]. For the interaction between the valence neutron and the proton target, we consider initially a simple Gaussian interaction
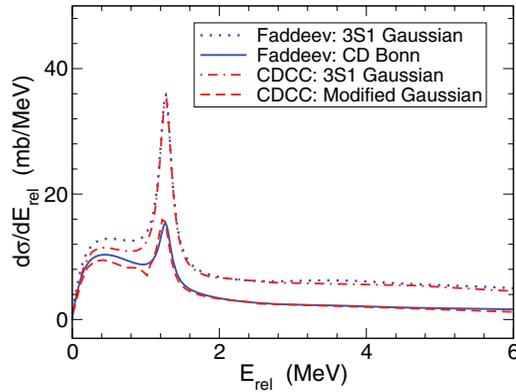
FIG. 2. (Color online) Differential cross section as a function of the n-^{10}Be relative energy calculated with the Faddeev/AGS and CDCC methods, using different choices for the valence neutron-proton interaction. The solid line is the Faddeev calculation using the realistic CD Bonn interaction. The dotted and dotted-dashed lines are, respectively, the Faddeev and CDCC calculations using a p-n Gaussian interaction adjusted to the $^{3}S_{1}$ s-wave phase-shifts: $V(r) = -72.15 \exp[-(r/1.484)^{2}]$. The dashed line is the CDCC calculations using the modified Gaussian interaction with the same geometry, but with the reduced strength $V_{0} = -45$ MeV. All these calculations ignore the ^{10}Be deformation.

$V(r) = -72.15 \exp[-(r/1.484)^{2}]$ [3], which reproduces the deuteron binding energy and low-energy s-wave triplet ($^{3}S_{1}$) phase shifts. The ^{11}Be continuum was discretized in energy intervals using the standard *binning* procedure. We included n-^{10}Be partial waves up to $\ell = 2$.

In Fig. 2 we represent the calculated energy spectrum $d\sigma/dE_{\text{rel}}$ that emerges by integrating the breakup cross section over the solid angle $d\Omega_{\text{c.m.}}$. To assess the reliability of the CDCC method in this case, we include also the Faddeev calculation (quoted from Ref. [23]), performed with the same two-body interactions. The CDCC calculation (dot-dashed line) reproduces fairly well the Faddeev result indicating that, at least in the limit of no-deformation, the CDCC is a reliable tool to analyze this reaction.

It was found by the authors of Ref. [23] that the breakup cross sections are very sensitive to the interaction between the valence neutron and the proton target. This is illustrated by the solid line in Fig. 2, which represents the Faddeev calculation performed replacing the simple Gaussian potential by the realistic CD Bonn interaction. This produces a sizable reduction of the breakup cross section. Consequently, to get reliable results it is mandatory to use a realistic nucleon-nucleon (NN) interaction. Unfortunately, existing implementations of the CDCC method do not incorporate the possibility of using these realistic NN interactions, such as Paris or CD Bonn. Nevertheless, we have found that the effect of using a realistic NN interaction can be well simulated reducing the depth of the Gaussian interaction to $V_{0} \approx -45$ MeV. The corresponding CDCC calculation, depicted by the dashed line in Fig. 2, is seen to reproduce fairly well the Faddeev result with the CD Bonn potential.

The corresponding angular distributions are shown in Fig. 3. The upper and bottom panels correspond to the relative
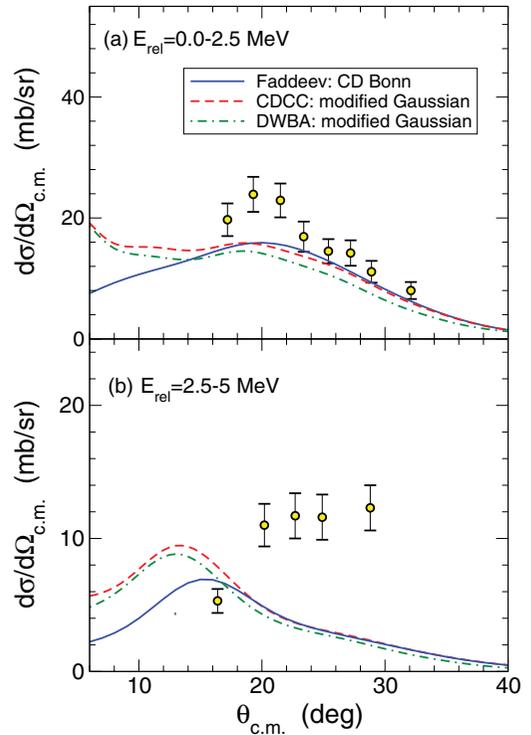

FIG. 3. (Color online) Angular distribution for the breakup of ^{11}Be on a proton target at 63.7 MeV/nucleon for $E_{\text{rel}} = 0$–2.5 MeV (upper panel) and $E_{\text{rel}} = 2.5$–5.0 MeV (bottom panel) calculated without deformation. The circles are the experimental data of Ref. [1]. The solid line is the Faddeev calculation with the realistic CD Bonn interaction. The dashed line is the CDCC calculation using the modified Gaussian interaction ($V_{g} = -45$ MeV) and the dot-dashed line is the CDCC calculation calculated in first order.

energy intervals $E_{\text{rel}} = 0$–2.5 MeV and $E_{\text{rel}} = 2.5$–5.0 MeV, respectively. In each panel, the solid line is the Faddeev calculation using the realistic CD Bonn interaction, whereas the dashed line is the CDCC calculation using the modified Gaussian potential. It is seen that both calculations are in reasonable agreement. There are discrepancies below 15°, where no data exist nevertheless. Since the calculations including deformation are performed within the DWBA approximation, we have included also in this plot the CDCC calculation performed in first order, which is equivalent to a DWBA calculation. It is seen that this calculation is very close to the full CDCC result, justifying the use of the Born approximation in this reaction. This plot shows also very clearly that the single-particle excitation mechanism is not adequate to describe these data, particularly in the higher excitation energy interval.

From the calculations presented in this section, we conclude that the CDCC method (even to first order), using an adequate effective p-n interaction, provides a good approximation to the more sophisticated Faddeev calculation with a realistic NN interaction. In the following section, we introduce the effect of core deformation using the C-ex model described in Sec. III.

B. Calculations with the core excitation model

To calculate the initial and final states of the projectile [Eqs. (26) and (27)] we adopt the valence-core potential from Ref. [25] (model Be12b) consisting of a central Woods-Saxon potential, with radius $R_0 = 2.483$ fm, diffuseness $a = 0.65$ fm, and parity-dependent depth, with $V_0 = -54.239$ MeV ($V_0 = -49.672$ MeV) for the even (odd) waves. This potential is deformed using a deformation parameter $\beta_2 = 0.67$, which corresponds to a deformation length of $\delta_2 = \beta_2 R_0 = 1.64$ fm. A spin-orbit term, using the standard Woods-Saxon derivative form for the radial shape, with the same radius and diffuseness as the central part and a depth of $V_{so} = 8.5$ MeV, is also included. For the ^{10}Be core we consider only the ground state (0^+) and the first excited state ($I^\pi = 2^+$, $E_x = 3.368$ MeV). The orbital angular momentum ℓ is truncated at $\ell_{max} = 3$. We considered continuum states with $J^\pi = 1/2^+$, $1/2^-$, $3/2^-$, $3/2^+$, and $5/2^+$.

With the assumed Hamiltonian and model space, the ground state corresponds predominantly to a $s_{1/2}$ configuration coupled to the core in the ground state ($\approx 85\%$), but with a significant admixture of the $|2^+ \otimes \nu d_{5/2}\rangle$ configuration ($\approx 13\%$).

This potential produces also the low-lying narrow resonances $5/2^+$, $3/2^-$, and $3/2^+$ at relative energies of 1.2, 2.7, and 3.2 MeV, respectively. These resonances can be identified with the states observed by Fukuda *et al.* in the ^{11}Be + ^{12}C reaction at 70 MeV/nucleon [19]. The $5/2^+$ resonance corresponds predominantly to a $d_{5/2}$ configuration coupled to the core in the ground state, whereas the $3/2^+$ resonance has a dominant ^{10}Be(2^+) $\otimes \nu s_{1/2}$ parentage.

For the interaction between the valence neutron and the proton target we use the modified Gaussian interaction obtained in the previous section. For the central part of the ^{10}Be $+$ p interaction we keep the Watson potential [24]. This interaction is used to calculate the distorted waves appearing in the DWBA transition amplitude. The noncentral part of this interaction, required to allow for the dynamic excitation of the core, is obtained deforming this central potential using the same deformation length ($\delta_2 = 1.64$ fm).

In Fig. 4 we show the calculated breakup cross section, as a function of the n-^{10}Be relative energy, integrated over the center-of-mass angular range $\theta_{c.m.} \leqslant 60°$. Figure 4(a) shows the contribution of the dominant J^π partial waves to the calculated energy spectrum, as well as the total sum of all included waves. It is seen that the breakup cross section is dominated by the resonant $3/2^+$ and $5/2^+$ contributions and, at low excitation energies, by the $3/2^-$ nonresonant continuum. The $1/2^-$ and $1/2^+$ waves (not shown in this figure) give also some contribution at small excitation energies. It is also observed that the $3/2^-$ resonance (located at $E_{rel} = 2.7$ MeV in this model) has a negligible effect on the cross section.

In Fig. 4(b), we show separately the valence and core excitation contributions to the angle-integrated breakup cross section. The low-energy spectrum is mostly due to the valence excitation, and hence the dynamic core excitation is negligible at these excitation energies. As the excitation energy increases the effect of core excitation becomes more and more important.
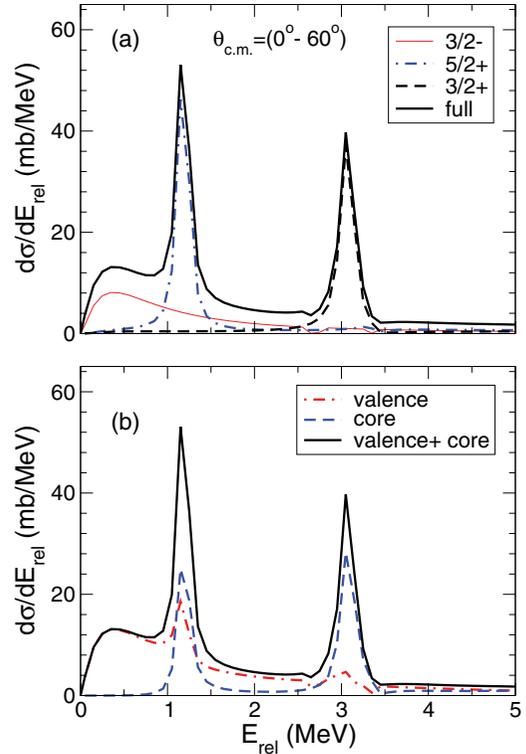

FIG. 4. (Color online) Differential energy cross section for $p(^{11}\text{Be},p)^{10}\text{Be}n$ at 63.7 MeV/nucleon integrated over the center-of-mass angular range $\theta_{c.m.} \leqslant 60°$, calculated with the C-ex model proposed in this work. The upper panel shows the individual contribution of the main partial waves and the sum of all included partial waves. The bottom panel shows the separate contribution coming from the valence excitation and dynamic core excitation amplitudes. See text for details.

In particular, core dynamic effects are clearly dominant in the region of the $3/2^+$ resonance and are also important in the region of the $5/2+$ resonance. We thus expect significant changes in the corresponding angular distributions.

In Fig. 5 we compare our results for the breakup cross section angular distribution $d\sigma/d\Omega_{c.m.}$ with the experimental data of Ref. [1] containing contributions within relative neutron–^{10}Be energy range 0–2.5 MeV [Fig. 5(a)] and 2.5–5 MeV [Fig. 5(b)]. Again, we show the separate contributions coming from the valence excitation (dot-dashed line) and dynamic-core excitation (dashed line), as well as their coherent sum (solid line). In the lower energy interval [Fig. 5(a)] the cross section is dominated by the single-particle breakup mechanism. The calculated angular distribution reproduces reasonably well the shape of the data, although some overestimation of the absolute magnitude is observed. On the other hand, in the higher energy interval [Fig. 5(b)], both the single-particle and dynamic core excitation mechanisms are important. The sum of both contributions accounts reasonably well for the data, except for the first data point, which is overestimated. The main contribution in this excitation energy region comes from the population of the $3/2^+$ resonance, as can be expected from Fig. 4. These results
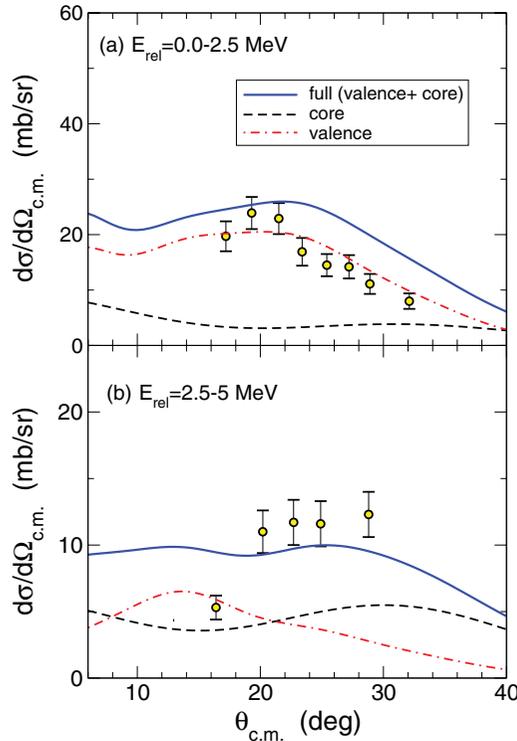
FIG. 5. (Color online) Angular distribution for the breakup of ^{11}Be on a proton target at 63.7 MeV/nucleon for $E_{rel} = 0$–2.5 MeV (upper panel) and $E_{rel} = 2.5$–5.0 MeV (bottom panel). The circles are the experimental data of Ref. [1]. The dashed-dotted and dashed curves represent the valence and core excitation contributions, respectively, whereas the solid line corresponds to their coherent sum.

evidence the importance of the core excitation mechanism and confirm our earlier findings using a more simplified model [17].

Finally, we note that this reaction has been studied also by the authors of Ref. [26] using an extended version of the CDCC method, which incorporates equivalent core excitation effects to those discussed here. However, contrary to our results, the effect of core excitation was found to be very small in that work. This result is unexpected given the large deformation of the ^{10}Be nucleus.

VI. CONCLUSION

In conclusion, we studied the problem of core excitation in the breakup scattering of halo nuclei. To account for this effect in a quantitative way, we developed a core excitation reaction model, based on the DWBA approximation, which takes into account the effect of core deformation in the structure of the halo nucleus, as well as the possibility of dynamic core excitation during the collision. We showed that, ignoring core-recoil effects, the contribution to the scattering amplitude arising from the core excitation can be written in terms of a superposition of two-body amplitudes corresponding to the inelastic scattering of the core scattered by the same target.

As an illustration of the model, we performed calculations for the breakup of ^{11}Be on protons at an incident energy of 63.7 MeV/nucleon. The initial and final states are treated within the particle-rotor model and hence they are considered as a superposition of several valence configurations coupled to the ^{10}Be core in either the ground state (0^+) or the first excited state (2^+). The noncentral part of the ^{10}Be + proton interaction, which is responsible for the dynamic core excitation, is obtained deforming the ^{10}Be + proton potential.

We find that the core excitation mechanism gives an important contribution and its inclusion permits a suitable description of the data from Ref. [1]. We also showed that the importance of dynamic core excitation becomes more important at increasing excitation energies and is in fact essential to account for the energy-integrated angular distribution at $E_{rel} = 2.5$–5.0 MeV.

From the calculations presented in this work, we may conclude that these core excitation effects will be also important in other reactions induced by weakly bound projectiles with deformed constituents. The method proposed here can provide a useful and simple estimate of these effects in those situations in which the assumptions of the model (i.e., the validity of the Born approximation and the possibility of neglecting core-recoil) are justified.

[1] A. Shrivastava *et al.* , Phys. Lett. B **596**, 54 (2004).

[2] Y. Satou *et al.*, Phys. Lett. B **660**, 320 (2008).

[3] N. Austern, Y. Iseri, M. Kamimura, M. Kawai, G. Rawitscher, and M. Yahiro, Phys. Rep. **154**, 125 (1987).

[4] P. Banerjee and R. Shyam, Phys. Rev. C **61**, 047301 (2000).

[5] J. A. Tostevin, S. Rugmai, and R. C. Johnson, Phys. Rev. C **57**, 3225 (1998).

[6] L. D. Faddeev, Zh. Eksp. Theor. Fiz. **39**, 1459 (1960) [Sov. Phys. JETP **12**, 1014 (1961)].

[7] E. O. Alt, P. Grassberger, and W. Sandhas, Nucl. Phys. B **2**, 167 (1967).

[8] S. Typel and G. Baur, Phys. Rev. C **50**, 2104 (1994).

[9] H. Esbensen and G. F. Bertsch, Nucl. Phys. A **600**, 37 (1996).

[10] T. Kido, K. Yabana, and Y. Suzuki, Phys. Rev. C **50**, R1276 (1994).

[11] S. Typel and G. Baur, Phys. Rev. C **64**, 024601 (2001).

[12] P. Capel, G. Goldstein, and D. Baye, Phys. Rev. C **70**, 064605 (2004).

[13] A. Garcia-Camacho, A. Bonaccorso, and D. M. Brink, Nucl. Phys. A **776**, 118 (2006).

[14] N. C. Summers, F. M. Nunes, and I. J. Thompson, Phys. Rev. C **74**, 014606 (2006).

[15] K. Horii, M. Takashina, T. Furumoto, Y. Sakuragi, and H. Toki, Phys. Rev. C **81**, 061602 (2010).

[16] R. C. Johnson, J. S. Al-Khalili, and J. A. Tostevin, Phys. Rev. Lett. **79**, 2771 (1997).

[17] R. Crespo, A. Deltuva, and A. M. Moro, Phys. Rev. C **83**, 044622 (2011).

[18] J. H. Kelley *et al.*, Nucl. Phys. A **880**, 88 (2012).

[19] N. Fukuda *et al*., Phys. Rev. C **70**, 054606 (2004).

[20] D. Brink and G. Satchler, *Angular Momentum*, 2nd ed., (Clarendon Press, Oxford, 1968).

[21] A. Bohr and B. Mottelson, *Nuclear Structure*, edited by W. A. Benjamin, (New York, 1969).

[22] I. Thompson, Comput. Phys. Rep. **7**, 167 (1988).

[23] E. Cravo, R. Crespo, A. M. Moro, and A. Deltuva, Phys. Rev. C **81**, 031601 (2010).

[24] B. A. Watson, P. P. Singh, and R. E. Segel, Phys. Rev. **182**, 977 (1969).

[25] F. M. Nunes, J. A. Christley, I. J. Thompson, R. C. Johnson, and V. D. Efros, Nucl. Phys. A **609**, 43 (1996).

[26] N. C. Summers and F. M. Nunes, Phys. Rev. C **76**, 014611 (2007).